ELSEVIER

Marine Geology 172 (2001) 167–180

MARINE GEOLOGY
INTERNATIONAL JOURNAL OF MARINE GEOLOGY, GEOCHEMISTRY AND GEOPHYSICS

www.elsevier.nl/locate/margeo

Reactive iron in Black Sea Sediments: implications for iron cycling

J.W.M. Wijsman, J.J. Middelburg*, C.H.R. Heip

Netherlands Institute of Ecology, Centre for Estuarine and Coastal Ecology, P.O. Box 140, 4400 AC Yerseke, The Netherlands

Received 1 February 2000; accepted 27 October 2000

Abstract

The distribution of reactive iron in sediments of the northwestern shelf, the shelf edge and the abyssal part of the Black Sea has been studied. In the euxinic Black Sea, iron sulfides (pyrite and iron monosulfide) are formed in the upper part of the anoxic water column and sink to the deep-sea floor where they are buried in the sediment. This flux of iron sulfides from the water column is reflected in enhanced concentrations of highly reactive iron and a high degree of pyritization (0.57–0.80) for the deep-water sediments of the Black Sea. The iron enrichment of deep-water sediments is balanced by a loss of highly reactive iron from the oxic continental shelf. Calculations from a numerical diagenetic model and reported in situ flux measurements indicate that the dissolved iron flux out of the shelf sediments is more than sufficient to balance the enrichment in reactive iron in deep-sea sediments, and that the majority of the dissolved iron efflux is redeposited on the continental shelf. This iron mobilization mechanism likely operates in most shelf areas, but its net effect becomes only apparent when reactive iron is trapped in sulfidic water bodies as iron sulfides or when iron is incompletely oxidized in low oxygen zones of the ocean and transported over long distances.

Keywords: Diagenesis; Sulfur; Modelling; Speciation; Pyrite; Euxinic basins

1. Introduction

The Black Sea is the world's largest permanently anoxic body of water and has been proposed as the modern equivalent of ancient euxinic basins (e.g. Berner and Raiswell, 1983; Berner, 1984; Calvert and Karlin, 1991; Lewis and Landing, 1991; Middelburg et al., 1991; Lyons and Berner, 1992; Lyons, 1997; Wilkin et al., 1997). Pyrite formation in euxinic basins is not limited to the sediment but also takes place in the upper reaches of the anoxic water column where dissolved sulfide is in contact with reactive iron phases (Goldhaber and Kaplan, 1974; Leventhal, 1983; Calvert and Karlin, 1991; Muramoto et al., 1991; Lyons, 1997; Wilkin et al., 1997). The production of pyrite in the water column and its settling to the sea floor leads to a decoupling of carbon and sulfur burial (Leventhal, 1983; Raiswell and Berner, 1985; Calvert and Karlin, 1991; Lyons and Berner, 1992), higher degrees of pyritization (Berner, 1970; Canfield et al., 1996) and higher reactive iron contents for euxinic sediments of the Black Sea compared to "normal" oxic marine sediments (Canfield et al., 1996; Raiswell and Canfield, 1998).

In marine deposits underlying oxic water, pyrite is formed in the sediments during early diagenesis (Goldhaber and Kaplan, 1974; Berner, 1984). In these sediments, sulfur concentrations are linearly related to the organic carbon content (Goldhaber and

* Corresponding author. Tel.: +31-113-577-476; fax: +31-113-573-616.

E-mail address: middelburg@cemo.nioo.knaw.nl (J.J. Middelburg).

0025-3227/01/$ - see front matter
PII: S0025-3227(00)00122-5

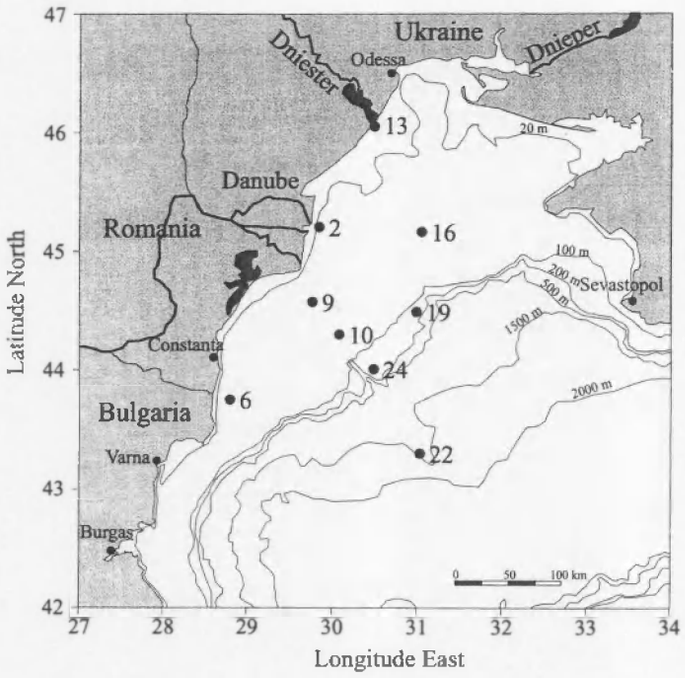

Fig. 1. Map of the northwestern Black Sea showing sampling locations.

Kaplan, 1974; Berner, 1984) because: (1) pyrite production is usually limited by the availability of biologically metabolizable organic matter (Berner, 1984); and (2) sulfide retention and carbon preservation are often coupled (Berner and Westrich, 1985). In euxinic basins, where iron sulfides form in the water column, pyrite production is to a certain degree decoupled from the amount of locally deposited sedimentary organic matter. In these systems, the availability of reactive iron is a more important factor limiting the production of pyrite (Raiswell and Berner, 1985; Boesen and Postma, 1988; Middelburg, 1991). This is often reflected in a lack of relation between concentrations of sulfur and organic carbon in these sediments (Berner and Raiswell, 1983; Leventhal, 1983; Calvert and Karlin, 1991; Lyons and Berner, 1992). Another indicator of iron-limitation for pyrite formation is the degree of pyritization (DOP) in the sediment. DOP indicates the extent to which "reactive" iron is present in the form of pyrite (Berner, 1970). The relatively high DOP values of deep-water sediments in the Black Sea and the absence of a relation between DOP and organic carbon content support the idea of iron-limitation fo pyrite formation (Raiswell and Berner, 1985; Calve and Karlin, 1991; Lyons and Berner, 1992).

Formation of pyrite in the upper reaches of th anoxic water column is also reflected in the reactiv iron enrichment relative to the total iron content o euxinic sediments (Canfield et al., 1996; Raiswell an Canfield, 1998). The term "reactive iron" refers to th iron fraction that is reactive towards dissolved sulfid at early diagenetic time scales, or is present in th form of pyrite (Berner, 1970; Goldhaber and Kaplan 1974; Raiswell and Canfield, 1998). Despite th generally high rates of sulfate reduction in coasta sediments, the abundance of reactive iron can prevei free sulfide from accumulating in the pore wate (Canfield, 1989; Raiswell and Canfield, 1998 However, in addition to the amount of reactive iron the time scale of reactivity is critical. Half-time reac tion rates of various sedimentary iron mineral with sulfide are known and vary over orders o magnitude (Canfield et al., 1992), and it is no possible to measure the concentration of most o these specific iron minerals in the sediment usin

Table 1
Sampling characteristics of the stations in the northwestern part of the Black Sea. Stations are grouped into 5 areas according to their geographical position. Oxygen concentration of the bottom water was measured by CTD, except data indicated by * that were measured in the overlying water of the box corer

Station	Location		Area	Depth (m)	Oxygen (μM)	Oxygen uptake (mmol O_2 m^{-2} d^{-1})[a]
	Latitude	Longitude				
2	45°12′N	29°51′E	Danube delta	26	207	37.9
6	43°45′N	28°48′E	Central shelf	52	285	14.0
9	44°34′N	29°46′E	Central shelf	57	243	11.6
10	44°18′N	30°05′E	Central shelf	72	284	11.0
13	46°03′N	30°29′E	Dniester delta	13	350	26.3
16	45°10′N	31°03′E	Central shelf	54	314*	10.0
19	44°29′N	31°00′E	Shelf edge	120	126*	6.1
22	43°18′N	31°02′E	Deep–sea	1494	0*	N.D.[b]
24	44°00′N	30°29′E	Shelf edge	137	190*	3.1

[a] Measured by deck incubations (for method description, see Wijsman et al., 1999).
[b] N.D., not determined.

standard techniques. However, they can be delineated through extraction into general "classes" of reactivity. A number of chemical extraction techniques have been used to subdivide the iron pool that is active on the time scale of early diagenesis (Lovley and Phillips, 1987; Canfield, 1989; Kostka and Luther, 1994; Raiswell et al., 1994). Based on such extraction procedures Raiswell and Canfield (1998), found that the euxinic sediments in the Black Sea are enriched in highly reactive iron compared to "normal" marine sediments deposited under an oxygenated water column. They also provided evidence for a small enrichment in highly reactive iron relative to total iron in euxinic Cariaco Basin sediments, but other euxinic systems such as the Orca Basin and Kau Bay were not enriched. Since Raiswell and Canfield (1998) had no data for the oxic continental shelf sediments, they could not show if this enrichment in highly reactive iron relative to total iron is restricted to the deep-sea or is characteristic of the Black Sea as a whole.

Previous studies in the Black Sea have focussed on the upper part of the anoxic water column (e.g. Lewis and Landing, 1991), the euxinic sediments of the deep-sea (e.g. Canfield et al., 1996; Lyons, 1997) or the sediments at the shelf edge, near the interface between oxic and anoxic bottom water (e.g. Shaffer, 1986; Lyons et al., 1993). In this study, special emphasis was paid to the oxic northwestern continental shelf area. This allows direct evaluation of reactive iron enrichment of Black Sea euxinic sediments relative to shelf settings. Moreover, assuming that the iron source to the Black Sea as a whole is not enriched in reactive iron relative to other marine systems, any enrichment of deep-water sediments should be balanced quantitatively by depletion in reactive iron of shelf sediments.

2. Sample collection and analysis

Nine stations of the 49th cruise of the R.V. *Prof. Vodyanitsky* spawning a range of sedimentological settings in the northwestern Black Sea were selected for this study (Fig. 1; Table 1). Stations 2 and 13 were situated just in front of the Danube and Dniester deltas, respectively. Stations 6, 9, 10 and 16 were located on the shallow central shelf. Two stations (19 and 24) were positioned near the oxic/anoxic interface on the shelf edge, and Station 22 was located in the euxinic deep basin with Unit I microlaminated sediments. Sediment was sampled using a Reineck box-corer ($60 \times 30 \times 30$ cm^3), and subcores were sliced with a resolution of 0.5–5 cm aboard ship inside a N_2-filled glove box. Sediments were stored frozen in diffusion-free bags under N_2-atmosphere until analysis.

The sediment was subjected to several chemical leaching experiments to determine various iron fractions: HCl extractable iron (FeH; cold 1 N

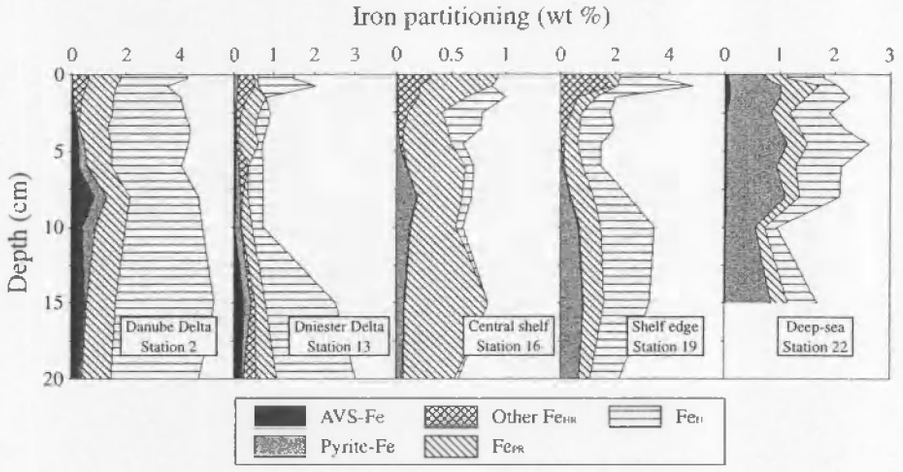

Fig. 2. Depth profiles of highly reactive iron present in acid-volatile sulfides (AVS), pyrite and other highly reactive (oxidized) iron sp poorly reactive iron and unreactive iron at representative stations in the Black Sea. All data are in units of weight percentage iron of the tot sediment. For station 22 no data were available for depths greater than 15 cm.

hydrochloric acid, 24 h) (Canfield, 1988; Canfield, 1989; Leventhal and Taylor, 1990; Raiswell et al., 1994), dithionite extractable iron (FeD; sodium dithionite 50 g l^{-1} in 0.2 M sodium citrate/0.35 M acetic acid, pH = 4.8, 2 h) (Canfield, 1988; Kostka and Luther, 1994) and total iron (FeT; microwave extraction with hydrochloric acid (12 N) and nitric acid (14 N)) This method for total iron extraction has been shown to be consistent with traditional total iron extractions involving HF (Nieuwenhuize et al., 1991). Iron from the HCl (FeH) and dithionite (FeD) extractions was determined spectrophotometrically using reducing ferrozine (Stookey and Ferrozine, 1970; Phillips and Lovley, 1987). The HCl extractions were measured directly, but the dithionite extractions were stored >1 day before adding reducing ferrozine in order to oxidize the dithionite, as recommended by Canfield et al. (1993). Total iron (FeT) was measured on a Perkin–Elmer atomic absorption spectrometer. Dithionite extracts iron from poorly and well crystallized iron oxides (except magnetite) as well as iron from AVS and carbonates and adsorbed onto sediment particles (Canfield, 1989; Canfield et al., 1993). HCl extracts the same iron fractions as dithionite with addition of poorly reactive iron silicates. Acid-volatile sulfides (AVS) were determined by means of a cold acid distillation with hydrochloric acid (6 N, 2 h) (Fossing and Jørgensen, 1989). Pyrite content was measured by the chromium re tion method (1 M Cr^{2+} in 4 N HCl, 2 h) (Zhabina Volkov, 1978; Canfield et al., 1986) after ace extraction to remove elemental sulfur (Passier et 1996). The liberated H_2S in the AVS and py extractions was stripped with N_2 gas and trappe de-oxygenated $Zn(Ac)_2$ (for a more detailed desc tion, see Wijsman et al., 2000) Fe in pyrite (FeP) AVS (FeAVS) was calculated from the sulfur con trations and mineral stoichiometry, assuming "F for AVS.

3. Results and discussion

3.1. Reactive iron

Raiswell and Canfield (1998) partitioned the to sediment iron pool into three operationally defi iron fractions with respect to their reactivity towa dissolved sulfide. Highly reactive iron (Fe_{HR}) is sum of the dithionite extractable iron (FeD) and iron that is present in the form of pyrite (FeP). Poo reactive iron (Fe_{PR}) is defined as the differer between the HCl extractable iron (FeH) and t dithionite extractable iron (FeD) and consists mair of iron silicates that are not very reactive towar sulfide (half life time $>10^5$ yr) on early diagene

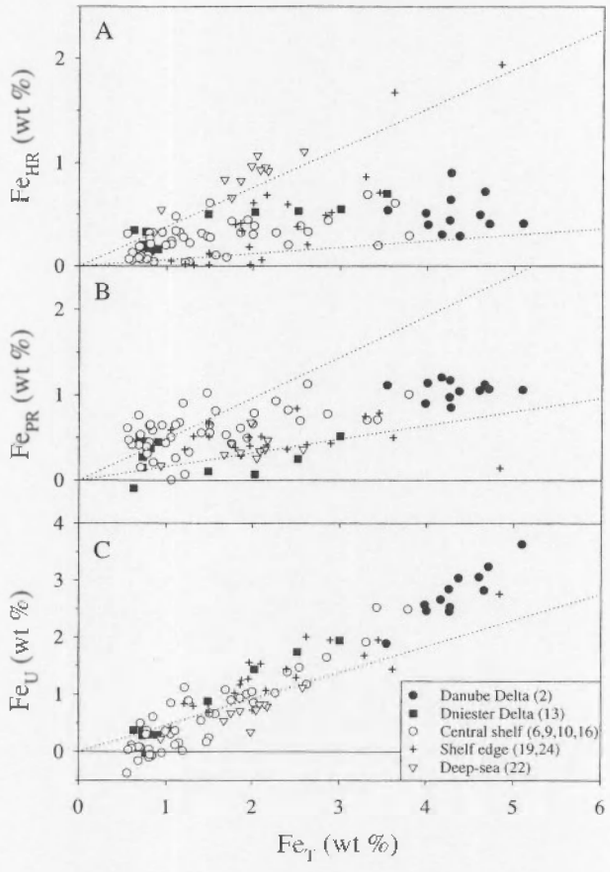

Fig. 3. Variations in the content of (A) highly reactive iron (Fe_{HR} = FeD + FeP), (B) poorly reactive iron (Fe_{PR} = FeH − FeD) and (C) unreactive iron (F_{eU} = FeT − FeH − FeP) with total iron in the sediments of the Black Sea. For each station within the various regions, the individual data for all sediment depths are presented. Dotted lines in (A) and (B) represent the upper and lower ranges, and the line in (C) represents the regression based on the comprehensive global data set of Raiswell and Canfield (1998) encompassing aerobic and dysaerobic continental shelf and deep-sea sediments. Station numbers are indicated between brackets.

time scales (Canfield et al., 1992). The unreactive iron (Fe_U) is defined as the total iron pool (FeT) minus the HCl-extractable iron (FeH) and the iron present in the form of pyrite (FeP).

Fig. 2 shows the partitioning of total iron over the various fractions as a function of depth in the sediments of stations 2, 13, 16, 19 and 22. The data for all stations are listed in Appendix 1. The shelf stations (2, 13, 16 and 19) were characterized by a surface peak of highly reactive iron, other than FeS and pyrite. These iron enrichments, probably composed of iron oxides, are either derived from sedimentation or from re-oxidation in the upper part of the sediment. The contribution of pyrite to the highly reactive fraction increased with depth at the expense of highly reactive iron oxides. The stations near the Danube and Dniester rivers (stations 2 and 13, respectively) were characterized by relatively high concentrations of AVS in the sediment, as is usually observed in rapidly accumulating sediments (Middelburg, 1991; Kostka and Luther, 1994; Gagnon et al., 1995; Lyons, 1997; Hurtgen et al., 1999). At the deep-sea station (22), pyrite was the dominant form of highly reactive iron, and oxidized forms were absent.

Fig. 3 shows the relationships between the highly reactive, poorly reactive and unreactive iron fractions and total iron for Black Sea samples together with the global trends derived by Raiswell and Canfield

Table 2
Summary of ratios of highly reactive iron content to total iron content (Fe_{HR}/FeT), measured in this study and as compiled by Raiswell and Canfield (1998)

Station	Average	S.E.	N
Delta area			
2	0.12	0.012	12
13	0.27	0.035	12
Total	0.19	0.024	24
Central shelf			
6	0.29	0.022	12
9	0.13	0.016	11
10	0.15	0.033	12
16	0.20	0.042	11
Total	0.20	0.017	46
Shelf–edge			
19	0.23	0.039	11
24	0.10	0.027	12
Total	0.16	0.027	23
Total shelf	0.19	0.012	93
Deep–sea			
22	0.47	0.018	10
Overall Black Sea	0.21	0.014	103
Raiswell and Canfield (1998)			
Continental margin	0.28	0.009	46
Deep Sea	0.25	0.013	56
Dysaerobic	0.28	0.020	26
All data	0.27	0.008	128

(1998). The latter are based on a comprehensive global data set of aerobic and dysaerobic continental margin and deep-sea sediments. The highest concentration of highly reactive iron (>1.5 wt%) was found in the upper cm of Station 19 located at the shelf edge. This enrichment, relative to total iron, is probably due to intensive recycling (remobilization) of iron by redox reactions near the sediment–water interface (Wijsman et al., 2000). The fraction of highly reactive iron in iron-rich sediments of the Danube delta ($Fe_{HR}/FeT = 0.12 \pm 0.012$ SE) is significantly lower (Students t-test, $p < 0.01$) compared to the Dniester delta sediments ($Fe_{HR}/FeT = 0.27 \pm 0.035$ SE) (Table 2). Sediments from the euxinic deep-water station 22 were enriched in highly reactive iron but not as pronounced as the non-turbidite Black Sea sediments of Raiswell and Canfield (1998). Nevertheless, the Fe_{HR}/FeT ratio at station 22 ranged from 0.38 to 0.58 (average 0.47 ± 0.018 SE), which is significantly higher (Students t-test, $p < 0.01$) than the data of Raiswell and Canfield (1998) for aerobic and dysaerobic marine environments. The highly reactive iron fraction at this deep-sea station was almost entirely composed of pyrite (97–100%; Fig. 2), which formed in the upper part of the anoxic water column (Muramoto et al., 1991; Lyons, 1997). The Fe_{HR}/FeT ratio in the non-turbiditic Black Sea sediments of Raiswell and Canfield (1998) ranged from 0.5 to 1. These higher ratios might be attributed to an overestimation of the FeD. Based on a cross-calibration with a small number of samples ($n = 5$), Raiswell and Canfield (1998) estimated that 38% of the HCl extractable iron is extractable by dithionite. However, in our deep-sea samples dithionite extractable iron contributed only 2.5% to the HCl extractable iron pool.

About 35% (±2.3% SE) of the total iron content in all our northwestern Black Sea sediments, was composed of poorly reactive iron. The shelf stations were enriched with poorly reactive iron compared to the continental margin sediments studied by Raiswell and Canfield (1998). Finally the unreactive iron content shows a linear relation with the total iron: $Fe_U = 0.72 \cdot FeT - 0.40$ ($n = 99$; $R^2 = 0.91$). The negative intercept indicates that at total iron concentrations lower than 0.56 wt% (= −intercept/slope = 0.4/0.72), the iron pool is entirely composed of reactive iron ($Fe_{HR} + Fe_{PR}$).

3.2. Degree of pyritization

The DOP has successfully been used as a marker for ancient euxinic sediments (Raiswell et al., 1988). It measures the extent to which reactive iron has been converted to pyrite and is usually calculated as:

$$DOP = \frac{FeP}{FeP + Fe^*}$$

where FeP is the iron present in the form of pyrite, and Fe^* is the reactive iron that has not yet reacted with sulfide. The reactive iron fraction (Fe^*) in the sediments is usually determined using a boiling HCl extraction (12 N, 1 min)(Berner, 1970) or a cold HCl extraction (1 N, 24 h; this study). The cold HCl extraction is suggested to yield DOP values for Black Sea sediments comparable to those of the traditional boiling HCl method (Leventhal and Taylor, 1990), but this does not necessarily hold for all type of

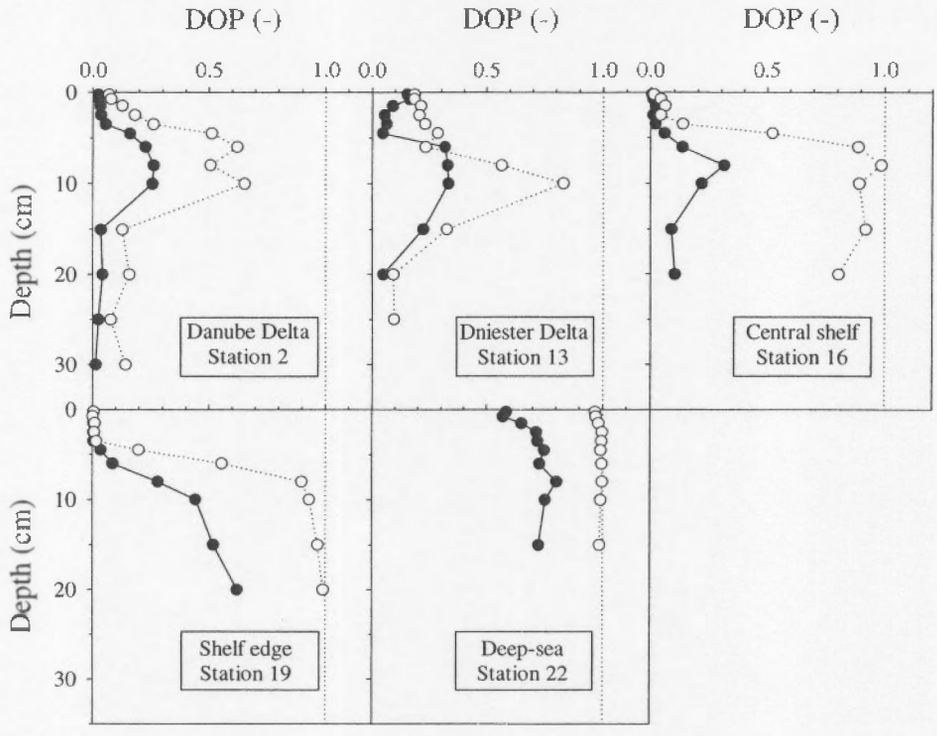

Fig. 4. Depth profiles of DOP_{HCl} (filled circles) and DOP_{Dith} (open circles) in the sediment at representative stations in the Black Sea. Dotted reference lines indicate DOP = 1, i.e. the situation where all the reactive iron has been converted into pyrite.

sediments. Typical values of DOP based on HCl extraction (DOP_{HCl}) are less than 0.42 for sediments deposited during oxygenated conditions, 0.42 to 0.8 for low oxygen environments and 0.55 to 0.93 for euxinic depositional conditions (Raiswell et al., 1988). In this study, the DOP_{HCl} values for the deep-sea Station 22 ranged from 0.57 in the upper part to 0.80 at depths $\geq\sim$10 cm in the sediment (Fig. 4), consistent with observations by Lyons and Berner (1992), Canfield et al. (1996), Calvert and Karlin (1991) and Lyons (1997). The slight increase with depth might result from the diagenetic component of pyrite formation (Lyons, 1997). The oxic shelf stations have lower DOP_{HCl} values ($<$0.4). However, at stations 19 and 24, located in the zone of alternating oxic and anoxic bottom water conditions (Lyons et al., 1993), the DOP_{HCl} increased to $>$0.5 at depths of more than 10 and 6 cm, respectively.

Due to the high sedimentation rates at the shallow water stations, their surficial sediments are relatively young compared to surficial sediments in the deep-sea. The processes of carbon degradation and pyrite formation at these shallow stations are not yet completed, and part of the reactive iron might still be converted to pyrite during burial, see Station 15 in Lyons (1997) and Hurtgen et al. (1999) for related observations. The degree of sulphidization (DOS; Boesen and Postma, 1988; Middelburg, 1991), calculated as:

$$DOS = \frac{FeP + FeAVS}{FeP + FeH}$$

yielded similar values as the DOP_{HCl} for stations 19, 22 and 24, which are poor in FeAVS. However, at the AVS-rich delta stations 2 and 13, DOS values were higher than the DOP_{HCl} values and ranged from 0.03 to 0.75. The abrupt decrease in DOP values at a depth of 10 cm probably results from a non-steady state deposition.

Suits and Wilkin (1998) introduced DOP_{Dith} in which dithionite extractable iron (FeD) is used as a measure of reactive iron because it extracts only a

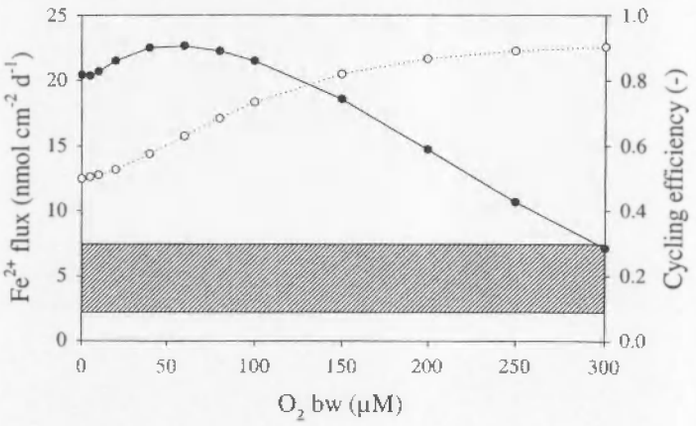

Fig. 5. Diagenetic model derived fluxes of dissolved iron into the water column (filled circles) and cycling efficiencies of iron in the sediment (open circles) as a function of the bottom water oxygen concentration. Hatched area indicates the range of net iron fluxes (2.22–7.44 nmol Fe cm^{-2} d^{-1}) that is required to sustain enrichment of highly reactive iron in the deep-sea.

small fraction of the poorly reactive iron silicates (Raiswell et al., 1994). At all stations, DOP_{Dith} approached unity at depths greater than 10 cm, except for the stations located in front of the river estuaries (Stations 2 and 13). Therefore, DOP_{Dith} values of subsurface sediments have limited power to resolve ancient bottom-water oxygen conditions.

3.3. The source of reactive iron

In contrast to the deep-sea sediments of the Black Sea, the shelf sediments were significantly depleted (Students t-test, $p < 0.01$) in highly reactive iron (Fe_{HR}/FeT ratio = 0.19 ± 0.012SE) compared to normal oxic and suboxic marine sediments in general (Raiswell and Canfield, 1998) (Table 2). This might be due to a re-allocation of highly reactive iron from the continental shelf to the deep-water euxinic sediments. A possible mechanism for this re-allocation is that dissolved iron, produced by iron reduction, is lost from the shelf sediments and subsequently transported to the chemocline in the euxinic part of the Black Sea. Lewis and Landing (1991) found elevated concentrations in dissolved iron in the upper part of the anoxic water column where pyrite formation occurs (Muramoto et al., 1991). The pyrite formed in the water column is lost from the system through sedimentation and burial in the sediment. Assuming that the microlaminated Station 22 is representative for the whole euxinic part of the Black Sea, this area is enriched in highly reactive iron by 0.24 and 0.81 wt% as compared to the upper and lower boundary, respectively, of the range characterizing normal aerobic and dysaerobic continental margin and deep-sea sediments (Raiswell and Canfield, 1998). This may represent an overestimate because turbiditic sediments cover only part of the basin and have lower reactive iron contents (Lyons, 1997). Based on a sediment accumulation rate of 0.02 cm yr^{-1} in the deep-sea area (Buesseler and Benitez, 1994) and an average porosity of 0.86 in the upper 15 cm, this results in a supplementary highly reactive iron flux of 0.82 to 2.75 nmol Fe cm^{-2} d^{-1}. Since the euxinic part covers 73% of the total area of the Black Sea (Sorokin, 1983), a net flux of 2.2 to 7.4 nmol Fe cm^{-2} d^{-1} is required from the continental shelf sediments to account for the enrichment in highly reactive iron in the deep-sea.

Oxygen present in the bottom water and in the upper few mm of the sediment column can possibly act as a trap for dissolved iron in the sediment. The reactive iron will then be recycled within the sediment through iron reduction at depth and iron oxidation and precipitation in the surface layer. We have investigated the influence of bottom water oxygen concentration on the internal cycling of iron and the dissolved iron flux out of the sediment by means of a numerical model for early diagenetic processes in Black Sea sediments (Wijsman et al., 2000). This

model explicitly resolves the major processes involved in sedimentary iron cycling. The parameter settings of Wijsman et al. (2000) were used, with a total depth integrated rate of mineralization (ΣR_{min}) of 1370 nmol C cm^{-2} d^{-1} and a reactive iron flux to the sediment ($J_{Fe(OH>)3}$) of 28 nmol cm^{-2} d^{-1}. The oxygen concentration in the bottom water was varied in the calculations between 0 and 300 μM. Fig. 5 shows the dissolved flux over the sediment–water interface and the cycling efficiency of iron (E) as a function of bottom-water oxygen concentrations. The cycling efficiency of iron is defined as:

$$E = \frac{R_{red}}{J_{Fe(OH)3} + R_{red}}$$

where R_{red} is the rate of iron reduction, and $J_{Fe(OH)3}$ is the flux of iron oxides to the sediment (Wijsman et al., 2000). At all bottom water oxygen levels, sulfate reduction is the dominant pathway for organic matter degradation. Under anoxic bottom-water conditions, the iron cycling efficiency is low (0.5), indicating that on average each mole of reactive iron arriving on the sediment is used once for iron reduction. The cycling efficiency of iron increases with increasing oxygen concentration in the bottom water, to a maximum value of 0.9 at an oxygen concentration of 300 μM. At this oxygen concentration, each iron molecule is reduced nine times before it is lost by burial or escapes into the water column. The calculated dissolved iron efflux reaches a maximum of 23 nmol cm^{-2} d^{-1} at a bottom-water oxygen concentration of about 50 μM. At lower oxygen concentrations, more iron is permanently buried in the sediment in the form of iron sulfides. At higher oxygen concentrations, the dissolved iron flux decreases to a minimum value of 7 nmol cm^{-2} d^{-1} because of a more efficient trapping in the surface layer. However, the trapping of iron in the surface layer is never complete, not even under fully oxygenated conditions. Friedl et al. (1998) and Friedrich et al. (2000) measured iron fluxes at 11 sites in the northwestern continental shelf using an in situ benthic flux chamber. Neglecting one extreme high value of 1633 nmol Fe cm^{-2} d^{-1} at the shelf edge (station BS26; Friedl et al., 1998), iron fluxes ranged from 0.5 to 184 (average 46) nmol Fe cm^{-2} d^{-1}.

The gross dissolved iron fluxes out of the sediment as calculated by the diagenetic model (7–22 nmol cm^{-2} d^{-1}; Fig. 5) and as measured in situ (average 46 nmol cm^{-2} d^{-1}) were higher than the net transfer of reactive iron from shelf sediments to the deep-sea predicted from reactive iron enrichment (2.4 to 7 nmol cm^{-2} d^{-1}). Clearly, the majority of the sedimentary iron efflux does not reach the deep-sea and is redeposited on the continental shelf. Most of the reduced iron diffusing out of sediments is rapidly oxidized and reprecipitated, but part of it may be transported laterally after incorporation in algae, bacteria or colloids (Schoeman et al., 1998). The northwestern shelf of the Black Sea is similar to other temperate continental shelf systems in terms of sediment characteristics and organic matter fluxes (Wijsman et al., 1999). The iron mobilization mechanism observed in the Black Sea likely operates in other shelf ecosystems as well, e.g. the North Sea and Californian shelf (Slomp et al., 1997; Johnson et al., 1999). Such an iron mobilization mechanism might be important to sustain high shelf productivity (Martin, 1990). The net effect of this iron mobilization mechanism becomes apparent only if: (1) there is a process driving (or facilitating) lateral transport; and (2) there is a sink of reactive iron. Both criteria are met in the Black Sea. The sulfidic water column and underlying sediments act as an efficient scavenger of any reactive iron being delivered, and there is significant transfer from the shelf to the interior of the Black Sea related to formation of the cold intermediate waters at the shelf (Tolmazin, 1985; Stanev, 1990; Oguz and Malanotte–Rizzoli, 1996). A similar mechanism may explain the transfer of dissolved iron from the shelf to the ocean interior in the low oxygen zones along the ocean margin. Landing and Bruland (1987) and Saager et al. (1989) clearly documented the importance of shelf mobilization and lateral transport in iron supply to the ocean interior. The mechanism underlying transfer of reactive iron (shelf-mobilization, lateral transport, and sulfide trapping) is generic, i.e. not specific to the Black Sea, and may be the key to understand ancient euxinic systems.

4. Conclusions

It has been suggested by Canfield et al. (1996) and Raiswell and Canfield (1998) that the formation of iron sulfides in the upper part of the anoxic water column of the Black Sea results in enrichment in

highly reactive iron of the deep-sea sediments. New data from the abyssal part of the Black Sea show that these sediments are indeed enriched in highly reactive iron. The flux of iron sulfides from the water column to the sea bottom is also reflected in the relatively high DOP values (0.57–0.80) in the deep-sea sediments. Additional data from the oxic continental shelf show that these sediments are depleted in highly reactive iron compared to other oxic and suboxic marine environments as summarized by Raiswell and Canfield (1998) (see Table 2). This depletion in reactive iron indicates that reactive iron is lost from these sediments. The total flux of dissolved iron from the sediments of the continental shelf into the water column is more than sufficient to balance for the burial of excess highly reactive iron in deep-sea sediments. The reported iron-transfer mechanism is generic and likely operates in most environments, but it is highly efficient in the Black Sea due efficient mechanisms for lateral transport and iron scavenging by sulfides.

Acknowledgements

We thank the chief scientist N. Panin and the crew of the RV *Professor Vodyanitsky* for logistic support and F. Meijsman and P. van Rijswijk for analytical assistance. We acknowledge G. Friedl and J. Friedrich for providing us with the data from the in situ benthic flux chamber. P. Herman, T. Lyons and S.E. Calvert are thanked for discussion and constructive reviews of the manuscript. This is publication no. 169 of the EU project EROS-21 (ENV4-CT96-0286) in the ELOISE program and publication no. 2692 of the Netherlands Institute of Ecology.

Appendix A

Depth distributions (cm) of various iron components and degree of pyritizations in northwestern Black Sea sediments. Total iron (FeT), HCl-extractable iron (FeH), dithionite-extractable iron (FeD),

Station	Depth	FeT	FeH	FeD	Fe_{HR}	Fe_{PR}	Fe_U	Pyrite	AVS	DOP_{HCl}	DOP_{Dith}
2	0–0.5	4.27	1.76	0.595	0.64	1.17	2.46	0.052	0.001	0.025	0.071
	0.5–1	3.54	1.61	0.494	0.54	1.11	1.89	0.049	0.001	0.026	0.079
	1–2	4.01	1.49	0.348	0.40	1.14	2.47	0.058	0.013	0.033	0.127
	2–3	4.17	1.45	0.249	0.30	1.20	2.66	0.063	0.053	0.036	0.180
	3–4	4.37	1.26	0.214	0.29	1.04	3.04	0.087	0.118	0.057	0.260
	4–5	4.26	1.19	0.215	0.44	0.97	2.85	0.259	0.154	0.159	0.511
	5–7	3.98	1.09	0.194	0.51	0.90	2.57	0.366	0.153	0.226	0.621
	7–9	4.28	1.29	0.444	0.90	0.85	2.53	0.524	0.492	0.261	0.506
	9–11	4.66	1.37	0.249	0.72	1.12	2.83	0.540	0.238	0.255	0.654
	14–16	5.10	1.41	0.357	0.41	1.06	3.63	0.060	0.303	0.036	0.128
	19–21	4.72	1.41	0.343	0.41	1.07	3.24	0.073	0.166	0.043	0.157
	24–26	4.61	1.51	0.456	0.50	1.05	3.06	0.045	0.276	0.025	0.078
	29–31	–	1.69	0.145	0.17	1.55	–	0.027	0.052	0.014	0.141
6	0–0.5	1.50	1.24	0.596	0.61	0.65	0.24	0.016	< 0.001	0.011	0.023
	0.5–1	1.15	0.97	0.298	0.32	0.67	0.16	0.028	0.002	0.025	0.076
	1–2	0.84	0.88	0.301	0.32	0.58	−0.06	0.025	0.011	0.024	0.067
	2–3	1.06	0.68	0.173	0.24	0.50	0.31	0.078	0.034	0.091	0.282
	3–4	1.11	0.78	0.133	0.34	0.65	0.12	0.238	0.038	0.209	0.608
	4–5	1.41	0.70	0.147	0.31	0.55	0.54	0.192	0.075	0.193	0.532
	5–7	0.80	0.60	0.156	0.31	0.44	0.04	0.182	0.039	0.209	0.503
	7–9	0.95	0.74	0.100	0.33	0.64	−0.02	0.261	0.039	0.234	0.695
	9–11	1.76	0.57	0.137	0.43	0.43	0.90	0.340	0.023	0.343	0.683
	14–16	0.80	0.71	0.070	0.26	0.64	−0.10	0.224	0.007	0.216	0.736
	19–21	1.94	0.54	0.047	0.45	0.49	1.00	0.459	0.003	0.425	0.895
	24–26	1.86	0.63	0.018	0.32	0.61	0.93	0.348	0.002	0.325	0.944
9	0–0.5	–	1.38	0.106	0.12	1.27	–	0.014	0.021	0.009	0.103

(*continued*)

Station	Depth	FeT	FeH	FeD	Fe_{HR}	Fe_{PR}	Fe_U	Pyrite	AVS	DOP_{HCl}	DOP_{Dith}
	0.5–1	1.57	0.90	0.084	0.10	0.81	0.66	0.023	0.022	0.022	0.193
	1–2	2.41	0.99	0.175	0.20	0.82	1.39	0.032	0.041	0.027	0.138
	2–3	3.43	0.86	0.149	0.20	0.71	2.53	0.055	0.057	0.053	0.244
	3–4	3.79	1.13	0.126	0.29	1.00	2.49	0.190	0.048	0.128	0.567
	4–5	2.63	1.21	0.081	0.33	1.12	1.18	0.288	0.024	0.172	0.756
	5–7	2.27	0.99	0.060	0.32	0.93	1.02	0.300	0.014	0.209	0.813
	7–9	2.00	0.71	0.048	0.30	0.66	1.04	0.294	0.007	0.266	0.842
	9–11	2.86	0.82	0.046	0.44	0.77	1.65	0.453	0.005	0.325	0.896
	14–16	3.31	0.72	0.013	0.69	0.70	1.92	0.779	0.003	0.486	0.981
	19–21	2.02	0.79	0.007	0.39	0.78	0.85	0.436	0.002	0.324	0.982
	24–26	3.63	–	0.018	0.61	–	–	0.678	0.005	–	0.971
	29–31	–	–	0.014	0.56	–	–	0.628	0.006	–	0.975
10	0–0.5	1.47	1.31	0.284	0.28	1.02	0.17	0.001	–	0.001	0.004
	0.5–1	1.51	0.83	0.274	0.28	0.56	0.67	0.001	< 0.001	0.001	0.002
	1–2	1.69	0.61	0.081	0.08	0.53	1.08	0.004	0.001	0.005	0.039
	2–3	1.26	0.37	0.039	0.04	0.33	0.89	0.004	0.002	0.009	0.077
	3–4	1.22	0.09	0.025	0.03	0.07	1.12	0.008	0.001	0.069	0.213
	4–5	0.85	0.22	0.010	0.04	0.21	0.60	0.036	0.001	0.126	0.754
	5–7	0.71	0.16	0.013	0.06	0.15	0.49	0.059	0.001	0.241	0.802
	7–9	1.06	0.02	0.012	0.21	0.00	0.85	0.227	0.001	0.925	0.942
	9–11	1.11	0.27	0.011	0.48	0.26	0.37	0.540	0.001	0.633	0.977
	14–16	1.19	0.91	0.005	0.28	0.90	0.02	0.312	0.001	0.231	0.980
	19–21	2.55	0.71	0.011	0.39	0.70	1.47	0.432	0.002	0.347	0.971
	24–26	1.27	–	0.006	0.22	–	–	0.247	0.002	–	0.972
13	0–0.5	1.49	0.51	0.410	0.50	0.10	0.88	0.105	0.001	0.151	0.182
	0.5–1	2.03	0.50	0.427	0.52	0.07	1.44	0.109	0.002	0.161	0.182
	1–2	0.76	0.72	0.262	0.33	0.45	−0.02	0.080	0.005	0.089	0.211
	2–3	0.90	0.58	0.130	0.16	0.45	0.29	0.038	0.013	0.055	0.204
	3–4	0.81	0.48	0.111	0.14	0.37	0.30	0.038	0.022	0.064	0.230
	4–5	0.69	0.58	0.070	0.10	0.51	0.08	0.032	0.016	0.046	0.285
	5–7	0.63	0.17	0.266	0.35	−0.09	0.37	0.092	0.026	0.317	0.231
	7–9	0.72	0.24	0.090	0.21	0.15	0.37	0.135	0.030	0.328	0.565
	9–11	0.73	0.30	0.030	0.18	0.27	0.28	0.172	0.010	0.331	0.832
	14–16	2.52	0.61	0.359	0.53	0.25	1.74	0.199	0.144	0.221	0.325
	19–21	3.00	1.01	0.498	0.55	0.51	1.94	0.059	0.104	0.048	0.093
	24–26	3.53	–	0.632	0.70	–	–	0.077	0.173	–	0.096
16	0–0.5	0.55	0.92	0.309	0.31	0.61	−0.37	0.004	< 0.001	0.004	0.012
	0.5–1	0.81	0.86	0.204	0.21	0.65	−0.05	0.010	< 0.001	0.010	0.042
	1–2	0.99	0.62	0.189	0.20	0.43	0.36	0.014	0.002	0.019	0.061
	2–3	0.78	0.41	0.097	0.10	0.31	0.37	0.005	0.004	0.010	0.042
	3–4	0.77	0.45	0.059	0.07	0.40	0.31	0.011	0.003	0.020	0.136
	4–5	0.61	0.46	0.026	0.05	0.44	0.11	0.033	0.001	0.058	0.523
	5–7	0.70	0.55	0.010	0.09	0.53	0.07	0.097	0.001	0.134	0.889
	7–9	0.69	0.41	0.003	0.19	0.41	0.09	0.215	< 0.001	0.312	0.986
	9–11	0.61	0.43	0.014	0.13	0.41	0.06	0.136	< 0.001	0.216	0.893
	14–16	0.68	0.77	0.006	0.08	0.76	−0.16	0.085	< 0.001	0.088	0.920
	19–21	0.57	0.48	0.013	0.07	0.47	0.03	0.063	< 0.001	0.102	0.806
19	0–0.5	3.61	2.16	1.666	1.67	0.50	1.44	0.011	–	0.004	0.006
	0.5–1	4.84	2.08	1.936	1.94	0.14	2.76	0.004	–	0.002	0.002
	1–2	2.01	1.28	0.603	0.61	0.68	0.72	0.007	< 0.001	0.005	0.010
	2–3	1.80	0.78	0.397	0.40	0.38	1.02	0.004	< 0.001	0.004	0.009

(*continued*)

Station	Depth	FeT	FeH	FeD	Fe_{HR}	Fe_{PR}	Fe_U	Pyrite	AVS	DOP_{HCl}	DOP_{Dith}
	3–4	1.96	0.69	0.180	0.18	0.51	1.27	0.004	0.001	0.004	0.017
	4–5	1.50	0.60	0.090	0.11	0.51	0.88	0.026	0.001	0.036	0.198
	5–7	1.49	0.74	0.056	0.13	0.68	0.69	0.080	< 0.001	0.086	0.556
	7–9	2.51	0.88	0.039	0.38	0.84	1.29	0.392	0.001	0.280	0.898
	9–11	3.45	0.83	0.049	0.71	0.78	1.96	0.760	0.001	0.442	0.932
	14–16	3.29	0.77	0.028	0.86	0.75	1.68	0.960	0.001	0.519	0.967
	19–21	2.16	0.41	0.006	0.69	0.41	1.07	0.783	0.001	0.621	0.991
22	0–0.5	1.75	0.45	0.022	0.66	0.43	0.67	0.734	0.038	0.586	0.967
	0.5–1	1.98	0.70	0.028	0.97	0.67	0.34	1.079	0.050	0.572	0.971
	1–2	2.18	0.48	0.016	0.92	0.47	0.79	1.042	0.055	0.652	0.982
	2–3	1.86	0.33	0.002	0.83	0.32	0.71	0.946	0.016	0.716	0.997
	3–4	2.14	0.37	0.005	0.95	0.36	0.83	1.092	0.019	0.721	0.995
	4–5	2.58	0.37	0.009	1.11	0.36	1.11	1.266	0.019	0.750	0.992
	5–7	2.09	0.34	0.004	0.93	0.34	0.82	1.065	0.013	0.730	0.996
	7–9	2.05	0.26	0.002	1.07	0.26	0.72	1.226	0.018	0.805	0.998
	9–11	0.94	0.17	0.005	0.54	0.17	0.22	0.621	0.010	0.755	0.992
	14–16	1.67	0.31	0.010	0.84	0.30	0.53	0.951	0.010	0.726	0.988
	19–21	1.64	0.26	–	–	–	–	–	–	–	–
	24–26	1.35	0.54	–	–	–	–	–	–	–	–
24	0–0.5	1.05	0.62	0.031	0.05	0.59	0.42	0.018	< 0.001	0.024	0.330
	0.5–1	1.21	0.37	0.015	0.02	0.36	0.84	0.003	< 0.001	0.006	0.133
	1–2	1.49	0.67	0.009	0.01	0.66	0.82	0.003	0.001	0.003	0.208
	2–3	1.31	0.52	0.007	0.01	0.51	0.79	0.001	< 0.001	0.002	0.130
	3–4	1.97	0.41	0.007	0.01	0.40	1.56	0.006	< 0.001	0.013	0.425
	4–5	2.10	0.52	0.013	0.06	0.51	1.54	0.049	0.001	0.076	0.761
	5–7	2.63	0.43	0.013	0.20	0.41	2.01	0.220	0.001	0.310	0.939
	7–9	1.88	0.30	0.005	0.34	0.29	1.25	0.383	0.001	0.529	0.986
	9–11	1.86	0.29	0.004	0.41	0.29	1.17	0.469	0.001	0.584	0.989
	14–16	2.40	0.37	0.008	0.60	0.36	1.44	0.677	0.003	0.613	0.986
	19–21	2.90	0.44	0.007	0.52	0.43	1.95	0.587	0.004	0.539	0.986
	24–26	2.83	–	0.008	0.49	–	–	0.556	0.008	–	0.983

highly reactive iron (Fe_{HR}), poorly reactive iron (Fe_{PR}) and unreactive iron (Fe_U) are given in wt% Fe. Pyrite and AVS are in wt% S.

References

Berner, R.A., 1970. Sedimentary pyrite formation. Am. J. Sci. 268, 1–23.

Berner, R.A., 1984. Sedimentary pyrite formation: An update. Geochim. Cosmochim. Acta 48, 605–615.

Berner, R.A., Raiswell, R., 1983. Burial of organic carbon and pyrite sulfur in sediments over Phanerozoic time: A new theory. Geochim. Cosmochim. Acta 47, 855–862.

Berner, R.A., Westrich, J.T., 1985. Bioturbation and the early diagenesis of carbon and sulfur. Am. J. Sci. 285, 193–206.

Boesen, C., Postma, D., 1988. Pyrite formation in anoxic environments of the Baltic. Am. J. Sci. 288, 575–603.

Buesseler, K.O., Benitez, C.R., 1994. Determination of mass accumulation rates and sediment radionuclide inventories in the deep Black Sea. Deep-Sea Res. 41, 1605–1615.

Calvert, S.E., Karlin, R.E., 1991. Relationships between sulphur, organic carbon, and iron in the modern sediments of the Black Sea. Geochim. Cosmochim. Acta 55, 2483–2490.

Canfield, D.E., 1988. Sulfate reduction and the diagenesis of iron in anoxic marine sediments. PhD Thesis, Yale University.

Canfield, D.E., 1989. Reactive iron in marine sediments. Geochim. Cosmochim. Acta 53, 619–632.

Canfield, D.E., Raiswell, R., Westrich, J.T., Reaves, C.M., Berner, R.A., 1986. The use of chromium reduction in the analysis of reduced inorganic sulfur in sediments and shales. Chem. Geol. 54, 149–155.

Canfield, D.E., Lyons, T.W., Raiswell, R., 1996. A model for iron deposition to euxinic Black Sea sediments. Am. J. Sci. 296, 818–834.

Canfield, D.E., Raiswell, R., Bottrell, S., 1992. The reactivity of sedimentary iron minerals towards sulfide. Am. J. Sci. 292, 659–683.

Canfield, D.E., Thamdrup, B., Hansen, J.W., 1993. The anaerobic degradation of organic matter in Danish coastal sediments: Iron reduction, manganese reduction, and sulfate reduction. Geochim. Cosmochim. Acta 57, 3867–3883.

Fossing, H., Jørgensen, B.B., 1989. Measurement of bacterial sulfate reduction in sediments: Evaluation of a single-step chromium reduction method. Biogeochemistry 8, 205–222.

Friedl, G., Dinkel, C., Wehrli, B., 1998. Benthic fluxes of nutrients in the northwestern Black Sea. Mar. Chem. 62, 77–88.

Friedrich, J., Dinkel, C., Friedl, G., Pimenov, N.V., Wijsman, J.W.M., Gomoiu, M.T., Cociasu, A.M., Popa, A., Wehrli, B., 2000. Benthic nutrient cycling and diagenetic pathways in the northwestern Black Sea. Estuar. Coast. Shelf Sci. (in press).

Gagnon, C., Mucci, A., Pelletier, É., 1995. Anomalous accumulation of acid-volatile sulphides (AVS) in a coastal marine sediment, Saguenay Fjord, Canada. Geochim. Cosmochim. Acta 59, 2663–2675.

Goldhaber, M.B., Kaplan, I.R., 1974. The sulfur cycle. In: Goldberg, E.D. (Ed.), Marine Chemistry. Wiley, New York, pp. 569–655.

Hurtgen, M.T., Lyons, T.W., Ingall, E.D., Cruse, A.M., 1999. Anomalous enrichments of iron monosulfide in euxinic marine sediments and the role of H_2S in iron sulfide transformations: examples from Effingham Inlet, Orca Basin, and the Black Sea. Am. J. Sci. 299, 556–588.

Johnson, K.S., Chavez, F.P., Friederich, G.E., 1999. Continental-shelf sediment as a primary source of iron for coastal phytoplankton. Nature 398, 697–700.

Kostka, J.E., Luther, G.W., 1994. Partitioning and speciation of solid phase iron in saltmarsh sediments. Geochim. Cosmochim. Acta 58, 1701–1710.

Landing, W.M., Bruland, K.W., 1987. The contrasting biogeochemistry of iron and manganese in the Pacific Ocean. Geochim. Cosmochim. Acta 51, 29–43.

Leventhal, J.S., 1983. An interpretation of carbon and sulfur relationships in Black Sea sediments as indicators of environmental deposition. Geochim. Cosmochim. Acta 47, 133–137.

Leventhal, J.S., Taylor, C., 1990. Comparison of methods to determine degree of pyritization. Geochim. Cosmochim. Acta 54, 2621–2625.

Lewis, B.L., Landing, W.M., 1991. The biochemistry of manganese and iron in the Black Sea. Deep-Sea Res. 38, S773–S803.

Lovley, D.R., Phillips, E.J.P., 1987. Rapid assay for microbially reducible ferric iron in aquatic sediments. Appl. Environ. Microbiol. 53, 1536–1540.

Lyons, T.W., 1997. Sulfur isotopic trends and pathways of iron sulfide formation in upper Holocene sediments of the anoxic Black Sea. Geochim. Cosmochim. Acta 61, 3367–3382.

Lyons, T.W., Berner, R.A., 1992. Carbon-sulfur-iron systematics of the uppermost deep-water sediments of the Black Sea. Chem. Geol. 99, 1–27.

Lyons, T.W., Berner, R.A., Anderson, R.F., 1993. Evidence for large pre-industrial perturbations of the Black Sea chemocline. Nature 365, 538–540.

Martin, J.H., 1990. Glacial–interglacial CO_2 change: the iron hypothesis. Paleoceanography 5, 1–13.

Middelburg, J.J., 1991. Organic carbon, sulphur, and iron in recent semi-euxinic sediments of Kau Bay, Indonesia. Geochim. Cosmochim. Acta 55, 815–828.

Middelburg, J.J., Calvert, S.E., Karlin, R.E., 1991. Organic-rich transitional facies in silled basins: Response to sea-level change. Geology 19, 679–682.

Muramoto, J.A., Honjo, S., Fry, B., Hay, B.J., Howarth, R.W., Cisne, J.L., 1991. Sulfur, iron and organic carbon fluxes in the Black Sea — sulfur isotopic evidence for origin of sulfur fluxes. Deep-Sea Res. 38, S1151–S1187.

Nieuwenhuize, J., Poley-Vos, C.H., Van Den Akker, A.H., Van Delft, W., 1991. Comparison of microwave and conventional extraction techniques for the determination of metals in soil, sediment and sludge samples by atomic spectrometry. Analyst 116, 347–351.

Oguz, T., Malanotte-Rizzoli, P., 1996. Seasonal variability of wind and thermohaline-driven circulation in the Black Sea: modeling studies. J. Geophys. Res. 101, 16 551–16 569.

Passier, H., Middelburg, J.J., Van Os, B.H.J., De Lange, G.J., 1996. Diagenetic pyritisation under eastern Mediterranean sapropels caused by downward sulphide diffusion. Geochim. Cosmochim. Acta 60(5), 751–763.

Phillips, E.J.P., Lovley, D.R., 1987. Determination of Fe(III) and Fe(II) in oxalate extracts of sediment. Soil Sci Soc Am J 51, 938–941.

Raiswell, R., Berner, R.A., 1985. Pyrite formation in euxinic and semi-euxinic sediments. Am. J. Sci. 285, 710–724.

Raiswell, R., Buckley, F., Berner, R.A., Anderson, T.F., 1988. Degree of pyritization of iron as a paleoenvironmental indicator of bottom-water oxygenation. J. Sediment. Petrol. 58, 812–819.

Raiswell, R., Canfield, D.E., 1998. Sources of iron for pyrite formation in marine sediments. Am. J. Sci. 298, 219–245.

Raiswell, R., Canfield, D.E., Berner, R.A., 1994. A comparison of iron extraction methods for the determination of degree of pyritisation and the recognition of iron-limited pyrite formation. Chem. Geol. 111, 101–110.

Saager, P.M., De Baar, H.J.W., Burkill, P.H., 1989. Manganese and iron in Indian Ocean waters. Geochim. Cosmochim. Acta 53, 2259–2267.

Schoeman, V., De Baar, H.J.W., De Jong, J.T.M., Lancelot, C., 1998. Effects of phytoplankton blooms on the cycling of manganese and iron in coastal waters. Limnol. Oceanogr. 43, 1427–1441.

Shaffer, G., 1986. Phosphate pumps and shuttles in the Black Sea. Nature 321, 515–517.

Slomp, C.P., Malschaert, J.F.P., Lohse, L., Van Raaphorst, W., 1997. Iron and manganese cycling in different sedimentary environments on the North Sea continental margin. Cont. Shelf Res. 17, 1083–1117.

Sorokin, Y.I., 1983. The Black Sea. In: Ketchum, B.H. (Ed.), Estuaries and Enclosed Seas. Elsevier, New York, pp. 253–292.

Stanev, E., 1990. On the mechanisms of the Black Sea circulation. Earth–Sci. Rev. 28, 285–319.

Stookey, L.L., Ferrozine, A., 1970. new spectrophotometric reagent for iron. Anal. Chem. 42, 779–781.

Suits, N.L., Wilkin, R.T., 1998. Pyrite formation in the water

column and sediments of a meromictic lake. Geology 26, 1099–1102.

Tolmazin, D., 1985. Changing coastal oceanography of the Black Sea. I: northwestern shelf. Prog. Oceanogr. 15, 217–276.

Wijsman, J.W.M., Herman, P.M.J., Gomoiu, M.T., 1999. Spatial distribution in sediment characteristics and benthic activity on the northwestern Black Sea shelf. Mar. Ecol. Prog. Ser. 181, 25–39.

Wijsman, J.W.M., Herman, P.M.J., Middelburg, J.J., Soetaert, K., 2000. A model for early diagenetic processes in sediments of the continental shelf of the Black Sea. Estuar. Coast. Shelf Sci. (in press).

Wilkin, R.T., Arthur, M.A., Dean, W.E., 1997. History of water-column anoxia in the Black Sea indicated by pyrite framboid size distributions. Earth Planet. Sci. Lett. 148, 517–525.

Zhabina, N.N., Volkov, I.I., 1978. A method of determination of various sulfur compounds in sea sediments and rocks. In: Krumbein, W.E. (Ed.), Methods, Metals and Assessment Vol. 3. Ann Arbor, MI, pp. 735–746.